IL NUOVO CIMENTO **47 C** (2024) 196
DOI 10.1393/ncc/i2024-24196-6

COLLOQUIA: HADRON2023

Dispersive calculation for $N^*(1520)$ transition form factors at low energies

D. AN(*)

Institutionen för fysik och astronomi, Uppsala universitet - Box 516, S-75120 Uppsala, Sweden

received 21 December 2023

Summary. — The transition form factors of $N^*(1520)$ have been formulated and computed at low energies ($|q^2| < 1$ GeV^2) using dispersion theory for the first time. Utilizing hadronic data from $N^*(1520) \to N\pi$, $N^*(1520) \to \Delta\pi$, and $N^*(1520) \to N\rho$ processes, we have calculated both space-like and time-like transition form factors. Our results demonstrate agreement with the existing space-like form factor data. The predicted time-like form factors can be experimentally tested by the HADES experiment.

1. – Introduction

Electromagnetic form factors (FFs) and transition form factors (TFFs) are important to understand the electromagnetic structure of nucleons. At high energies where perturbative QCD applies due to asymptotic freedom, the minimal quark content is prevalent [1, 2] and the asymptotic behavior can be estimated using, for example, quark counting rules. At low energies (large distances), the structure of hadrons is sensitive to the excitations of pions, because the pions are extraordinarily light. Their small masses are related to the spontaneous breaking of chiral symmetry, which gives rise to the pions as Goldstone bosons. It is the intermediate energy range that remains the least understood part. An interesting and deeper question to ask is: how should one understand *quantitatively* and *model-independently* the FFs and TFFs from first principles in the intermediate energy range where the perturbative QCD fails and other hadronic degrees of freedom are excited (*e.g.*, Δ, ρ meson)? To answer this question, dispersion theory together with chiral perturbation theory (ChPT) can be applied. The purpose of this project and related ones [3-5] is to improve on the description of these long-range pionic effects as one part of the structure information of the composite hadronic states.

(*) E-mail: di.an@physics.uu.se

While studying in [3-5] ground state baryons we will address here the lowest-lying excitation of the nucleon with negative parity, the $N^*(1520)$.

2. – Dispersion relations

The $N^*(1520)$ has iso-spin $I = 1/2$ and $J^P = 3/2^-$ [6]. The electromagnetic matrix element is given by

$$\langle N|j_\mu|N^*\rangle = e\,\bar{u}_N(p_N)\,\Gamma_{\mu\nu}(q)\,u^\nu_{N^*}(p_{N^*}) \tag{1}$$

with

$$\Gamma^{\mu\nu}(q) := i\left(\gamma^\mu q^\nu - \not{q} g^{\mu\nu}\right) m_N F_1(q^2) + \sigma^{\mu\alpha} q_\alpha q^\nu F_2(q^2) + i\left(q^\mu q^\nu - q^2 g^{\mu\nu}\right) F_3(q^2), \tag{2}$$

where $q^\mu := p^\mu_{N^*} - p^\mu_N$ and F_i are TFFs with $i = 1, 2, 3$. The TFFs F_i are constructed based on the Bardeen-Tung-Tarrach construction (BTT construction) [7, 8]. Therefore they are constraint-free and qualify for a dispersive representation. Diagramatically, they are represented by the grey blob in fig. 1.

If one writes the S-matrix (schematically) as $S = 1 + iT$ with the matrix T including the true scattering amplitudes, then the unitarity of S leads to the optical theorem here applied to nucleon TFFs,

$$\mathrm{Im}T_{\gamma^*\to N^*\bar{N}} \sim \sum_i T_{\gamma^*\to i}\left(T^\dagger\right)_{i\to N^*\bar{N}}, \tag{3}$$

where the intermediate states i cover 2π, 3π, 4π, ..., $K\bar{K}$, $K\bar{K}\pi$, ..., $N\bar{N}$, ... From the S-matrix point of view, the importance of intermediate states is ordered by their threshold. At low energies, the most important state is 2π. We restrict ourselves to the iso-vector FFs and $|q^2| < 1\,\mathrm{GeV}^2$, thus the 3π state will not be considered. For more than 3 pions, the Goldstone theorem requires that the couplings of pion fields are suppressed by the derivative couplings which pushes their importance to higher energies ($q^2 > m_\rho^2$). Note that the sum is restricted to asymptotic states and hadronic resonances do not appear in the intermediate states but rather phase shifts. From a phenomenological point of view, the 2π state includes the ρ meson in the phase shifts. We further approximate the BM blob in fig. 1, which contains baryonic and mesonic interaction, by including nucleon and the Δ in the cross-channels. The Δ has been shown to be important, both phenomenologically and also in large-Nc QCD where Δ becomes even degenerate with the nucleon [3, 4].

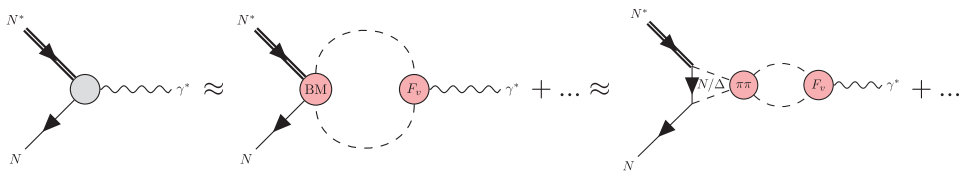

Fig. 1. – Dispersive machinery for the TFFs at low energy. Dashed lines are pions. The BM blob stands for Baryon and Meson interaction.

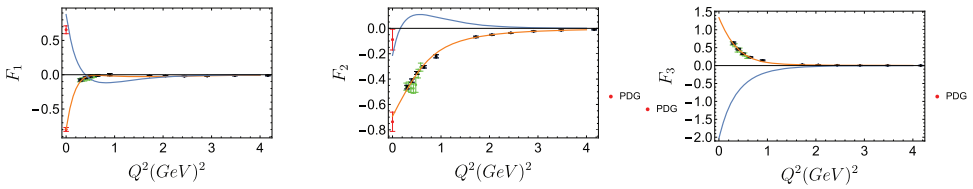

Fig. 2. – Orange: Lisbon parametrization [9] for proton; blue: MAID parametrization for neutron [10, 11]. Green and black data points are proton Jlab data [12-14]. Data at $Q^2 = 0$ are taken from the PDG [6].

The dispersion relations are formulated for the constraint-free TFFs,

$$F_i(q^2) = \frac{1}{12\pi} \int_{4m_\pi^2}^{\infty} \frac{\mathrm{d}s}{\pi} \frac{T_i(s)\, p_{\mathrm{cm}}^3(s) F_v^*(s)}{s^{1/2}\,(s - q^2 - i\epsilon)} + F_i^{\mathrm{anom}}(q^2) + \ldots, \tag{4}$$

where $T_i(s) \sim \langle 2\pi | N^* N \rangle$ represents the hadronic p-wave amplitudes. $F_v(s)$ is the pion vector form factor. The contribution $F_i^{\mathrm{anom}}(q^2)$ on the right-hand side of eq. (4) comes from the anomalous cut in the complex plane. The details of the anomalous cut can be found in [5]. Using the Muskhelishvili-Omnès framework $T_i(s)$ is calculated dispersively as

$$T_i(s) = K_i(s) + \Omega(s)\, P_i + T_i^{\mathrm{anom}}(s) + \Omega(s)\, s \int_{4m_\pi^2}^{\infty} \frac{\mathrm{d}s'}{\pi} \frac{K_i(s')\, \sin\delta(s')}{|\Omega(s')|\,(s' - s - i\epsilon)\, s'}, \tag{5}$$

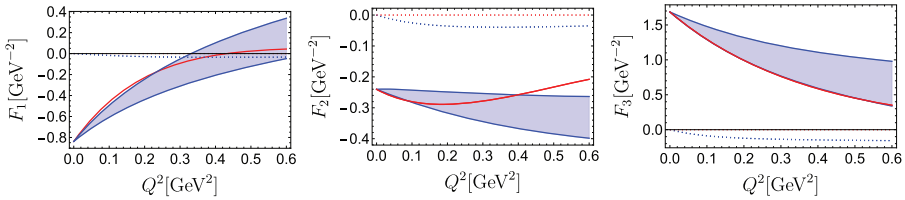

Fig. 3. – Red: parametrization for iso-vector TFFs using Lisbon parametrization for proton, the MAID parametrization for neutron. Blue: this work (preliminary). Full lines: real part; dashed lines: imaginary part.

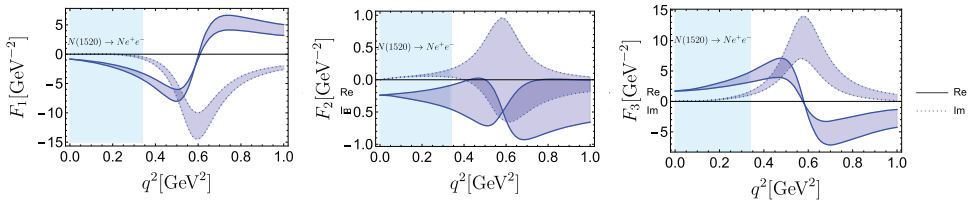

Fig. 4. – Time-like transition FFs (preliminary). Full lines: real part; dashed lines: imaginary part. The experimentally accessible region given by $q^2 \in [4m_e^2, (m_N - m_{N^*})^2]$ which corresponds to the shaded area.

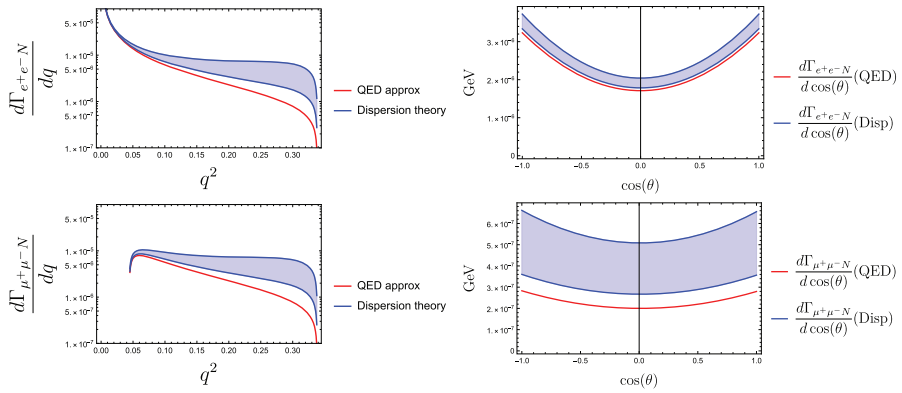

Fig. 5. – Predictions for electronic and muonic differential decay width (preliminary).

where $T_i(s)$ is decomposed into the left-hand cut $K_i(s)$ and the rest contains the right-hand cuts. We obtain K from chiral perturbation theory together with effective Lagrangian containing $N(1520)$-N-π and $N(1520)$-Δ-π interaction. P_i are subtraction constants that physically parametrize the high-energy contributions that are not explicitly covered by the dispersive framework. The subtraction constants therefore are fixed to match $N^* \to N\rho$ decay widths [6].

3. – Results (preliminary) and outlook

We define the isovector form factors as $F_i^v = \frac{1}{2}(F_i^p - F_i^n)$. The proton $F_i^p(Q^2)$ and neutron $F_i^n(Q^2)$ in the space-like region are shown in fig. 2 where one can see that $F_i^p(Q^2) \approx -F_i^n(Q^2)$ for $i = 1, 3$ in the low-energy region, meaning that the $N^*(1520)$ is iso-vector dominated for $i = 1, 3$. Our preliminary results for the space-like FFs are shown in fig. 3 where one sees a nice agreement with the iso-vector TFF estimates (red curve). The time-like form factors are shown in fig. 4. The experimentally accessible

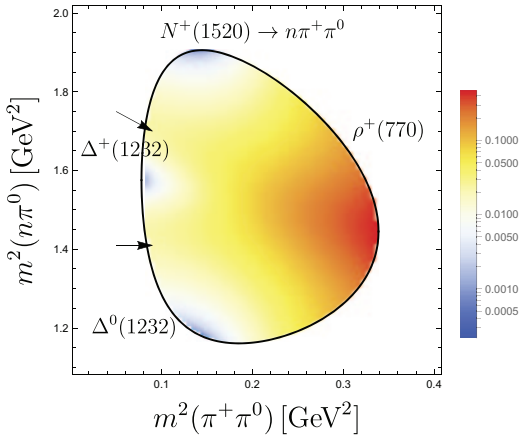

Fig. 6. – Dalitz plot $\frac{d\Gamma}{dm^2(n\pi^0)dm^2(\pi^+\pi^0)}$ for $N^*(1520) \to n\pi^+\pi^0$ (preliminary).

region is shaded in blue which one can probe by measuring $N^*(1520) \to Nl^+l^-$, $l = e, \mu$. The differential Dalitz decay is predicted for electrons and muons, respectively, in fig. 5.

For the iso-vector dominated $N^*(1520)$ resonance, the TFFs are closely related to the $N^* \to N2\pi$ decays. Having fixed all the parameters using the hadronic data $N^*(1520) \to N\pi, \Delta\pi, N\rho$ in our framework, we make predictions for the hadronic Dalitz decay $N^* \to N2\pi$ using the dispersion relations of eq. (5). In fig. 6, the double differential Dalitz plot is shown. Three resonances can be seen in the Dalitz plot: Δ^0, Δ^+, and ρ meson. Our prediction for the TFFs and the hadronic Dalitz decay can be tested by the HADES experiment in the future. More accurate experimental input for $N^*(1520) \to N\rho, N\pi, \Delta\pi$ decays and better measurement on the neutron TFFs in the low-Q^2 region will help to reduce our theoretical uncertainty.

* * *

This work has been supported by the Swedish Research Council (Vetenskapsrådet) (grant No. 2019-04303).

REFERENCES

[1] Brodsky Staley J. and Farrar Glennys R., *Phys. Rev. D*, **11** (1975) 1309.
[2] Lepage G. Peter and Brodsky Staley J., *Phys. Lett. B*, **87** (1979) 359.
[3] Granados Carlos, Leupold Stefan and Perotti Elisabetta, *Eur. Phys. J. A*, **53** (2017) 117.
[4] Leupold Stefan, *Eur. Phys. J. A*, **54** (2018) 1.
[5] Junker Oloy, Leupold Stefan, Perotti Elisbetta and Vitos Timea, *Phys. Rev. C*, **101** (2020) 015206.
[6] Workman R. L. *et al.*, *PTEP*, **2022** (2022) 083C01.
[7] Bardeen William A. and Tung W. K., *Phys. Rev.*, **173** (1968) 1423; **4** (1971) 3229(E).
[8] Tarrach R., *Nuovo Cimento A*, **28** (1975) 409.
[9] Eichmann Gernot and Ramalho G., *Phys. Rev. D*, **98** (2018) 093007.
[10] Tiator L., Drechsel D., Kamalov S. S. and Vanderhaeghen M., *Chin. Phys. C*, **33** (2009) 1069.
[11] Tiator L., Drechsel D., Kamalov S. S. and Vanderhaeghen M., *Eur. Phys. J. ST*, **198** (2011) 141.
[12] Aznauryan I. G. *et al.*, *Phys. Rev. C*, **80** (2009) 055203.
[13] Mokeev V. I. *et al.*, *Phys. Rev. C*, **93** (2016) 025206.
[14] Mokeev V. I. *et al.*, *Phys. Rev. C*, **86** (2012) 035203.